

AD-A152 090

PLASTIC DEFORMATION OF CRYSTALLINE POLYMERS(U) AKRON
UNIV OH INST OF POLYMER SCIENCE A N GENT ET AL. MAR 85
TR-36-15 N00014-76-C-0408

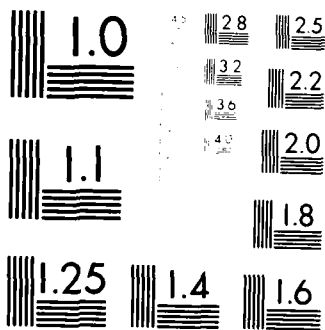
1/1

UNCLASSIFIED

F/G 11/9

NL

							END							
							10/80							
							870							



MICROCOPY RESOLUTION TEST CHART
NATIONAL BUREAU OF STANDARDS-1963-A

②

AD-A152 090

OFFICE OF NAVAL RESEARCH
Contract N00014-76-C-0408
Project NR 092-555

Technical Report No. 36

PLASTIC DEFORMATION OF CRYSTALLINE POLYMERS

by

A. N. Gent and Jongkoo Jeong

Institute of Polymer Science
The University of Akron
Akron, Ohio 44325

DTIC
ELECTE
APR 8 1985
S D
B

March, 1985

Reproduction in whole or in part is permitted for
any purpose of the United States Government

Approved for Public Release; Distribution Unrestricted

DTIC FILE COPY

85 03 21 165

REPORT DOCUMENTATION PAGE		READ INSTRUCTIONS BEFORE COMPLETING FORM
1. REPORT NUMBER Technical Report No. 36	2. GOVT ACCESSION NO. A152090	3. RECIPIENT'S CATALOG NUMBER
4. TITLE (and Subtitle) Plastic Deformation of Crystalline Polymers	5. TYPE OF REPORT & PERIOD COVERED Technical Report	
	6. PERFORMING ORG. REPORT NUMBER	
7. AUTHOR(s) A. N. Gent and Jongkoo Jeong	8. CONTRACT OR GRANT NUMBER(s) N00014-76-C-0408	
9. PERFORMING ORGANIZATION NAME AND ADDRESS Institute of Polymer Science The University of Akron Akron, Ohio 44325	10. PROGRAM ELEMENT, PROJECT, TASK AREA & WORK UNIT NUMBERS NR 092-555	
11. CONTROLLING OFFICE NAME AND ADDRESS Office of Naval Research Power Program Arlington, VA 22217	12. REPORT DATE March, 1985	
	13. NUMBER OF PAGES 31	
14. MONITORING AGENCY NAME & ADDRESS (if different from Controlling Office)	15. SECURITY CLASS. (of this report) Unclassified	
	15a. DECLASSIFICATION/DOWNGRADING SCHEDULE	
16. DISTRIBUTION STATEMENT (of this Report) According to attached distribution list. Approved for public release; distribution unrestricted.		
17. DISTRIBUTION STATEMENT (of the abstract entered in Block 20, if different from Report)		
18. SUPPLEMENTARY NOTES Submitted for publication in: Polymer Engineering and Science		
19. KEY WORDS (Continue on reverse side if necessary and identify by block number) Crystalline polymers, Deformation, Drawing, Ductility, Plastic deformation, Polyethylene, Polymers.		
20. ABSTRACT (Continue on reverse side if necessary and identify by block number) Draw ratios have been measured for samples of polyethylene and trans-polyisoprene, crystallized at various temperatures and at various degrees of orientation. The values obtained range from unity, i.e., no drawing is observed, up to values of about 15X for materials crystallized in the oriented state and then drawn in a perpendicular direction. The results are in rough accord with a simple molecular network model in		

1. Introduction

One of the most remarkable features of partially-crystalline polymers is their ability to undergo large plastic deformations ("drawing") without rupture. This phenomenon is readily distinguished from plastic yielding in ductile metals, which is considerably smaller in extent, or in glassy polymers, where yielding is localized within narrow shear bands. In contrast, plastic yielding in partially-crystalline polymers takes place in a relatively homogeneous way and results in deformations of several hundred percent without rupture(1). The material then strain hardens after drawing so that further deformation is only achieved by imposing higher stresses.

Representative relations between tensile stress and displacement of the clamps securing a tensile specimen are shown in Figures 1 and 2. After the yield stress σ_y is reached the specimen spontaneously thins over part of its length to form a "neck" where the extension is large. The rest of the specimen is still lightly stretched. Further displacement of the clamps is achieved by an increase in the amount of material in the neck at the expense of the lightly-strained material on either side of it. This transformation continues at a constant stress, generally smaller than σ_y , until the whole specimen has become uniformly stretched to the "natural draw ratio", i.e., the stretch ratio set up in the neck, denoted here d.

The natural draw ratio, as discussed in more detail later, is quite different for different polymers. For example, low-density polyethylene (LDPE) can only be drawn to about 5 times its original length whereas high-density polyethylene (HDPE) can be drawn 10X - 12X. Moreover, the draw ratio depends to a considerable degree upon the conditions under which crystallization took place, being much smaller for polymers crystallized in an oriented state.

Although considerable attention has been given to the molecular structure of semi-crystalline polymers and the rearrangements that accompany plastic yielding and drawing (2,3), relatively little work has been published on quantitative aspects of the drawing process. Some preliminary observations are therefore reported here of the extent of plastic deformation that various crystalline polymers will undergo, and of the effect of the mode of crystallization upon their subsequent deformability. An attempt is then made to account for the marked differences observed in deformability between different polymers, and between different crystallization conditions for the same polymer, in terms of a simple model of the drawing process.

2. Experimental Details

(i) Materials

Samples were prepared in the form of molded sheets about 2 mm thick from several materials: trans-polyisoprene (TPI), supplied by Polysar Limited, denoted TP-301; high-density polyethylene (HDPE-1), supplied by Asahi-Kasei Industries, denoted Microsuntec R340P; a second sample of molding-grade high-density polyethylene (HDPE-2) supplied by Union Carbide Corporation, denoted 8908; a sample of pipe-grade medium-density polyethylene (MDPE) supplied by Union Carbide Corporation, denoted E608; and a sample of film-grade low-density polyethylene (LDPE), also supplied by Union Carbide Corporation and denoted DFDY 0774. Trans-polyisoprene (TPI) was also examined in the lightly-crosslinked state, brought about by adding 1 percent by weight of dicumyl peroxide and 1 percent of an antioxidant (Antioxidant 2246, American Cyanamid Company) to the material before hot-pressing for 1 h at 150°C. The crosslinked material is denoted TPI-X.

Samples of HDPE-1 and TPI-X were crystallized in the oriented state by melting the molded sheets at 160°C and 95°C, respectively, for 15 minutes and then rapidly stretching them to a predetermined length. They were then cooled rapidly in the stretched state so that crystallization

took place completely before release. The exact state of orientation was determined from the dimensions of an inked grid applied to the molded sheet initially.

Measured values of the density \underline{d} of the crystallized sheets and values of the degree of crystallinity \underline{C} calculated from them are given in Table 1. No significant changes in \underline{d} and hence \underline{C} were observed with the extent of orientation imposed during crystallization.

(ii) Determination of draw ratio

When a specimen deforms by cold drawing, the extension becomes highly non-uniform until the whole sample has been transformed into the drawn state. Further deformation then occurs homogeneously under increasing stress up to the point of rupture. The natural draw ratio is that set up in the necked region before the onset of strain hardening and subsequent uniform deformation. It was measured by the separation of grid lines placed on the sample initially. The measurements were made while the samples were under tension and in the process of being drawn.

Typical tensile stress-strain relations are shown in Figures 1 and 2 for oriented test pieces of HDPE-1 and TPI-X, stretched at a nominal strain rate of 0.05 s^{-1} at 25°C . When the stretching direction was at right angles to the direction of prior orientation, represented by an extension

ratio λ , then the corresponding value of extension ratio in the direction of extension, given by λ^{-1} , was less than unity. Values of the extension ratio in the direction of subsequent stretching have been employed in Figures 1 and 2 to characterize the degree of prior orientation imposed during crystallization.

3. Experimental Results

(i) Stress-strain relations

Necking and drawing took place when the prior orientation ratio λ was less than about 8 for HDPE-1 and less than about 2 for TPI-X, Figures 1 and 2. For greater amounts of prior orientation a distinctly different type of deformation occurred. No signs of necking were observed and, instead of a pronounced drop in tensile load at the yield point, only a change in slope of the load-displacement relation was noted, Figures 1 and 2.

Measured values of the yield stress σ_Y are plotted in Figure 3 against the pre-orientation ratio λ . For HDPE-1 they did not change significantly over the entire range of orientation, being about 24 MPa, and for TPI-X only a slight increase was found, from about 9 to 14 MPa, as the degree of prior orientation increased. The difference in σ_Y between the two

polymers may be due largely to the different levels of crystallinity; 65 percent and 36 percent, respectively. Changes in crystallite orientation or microstructure brought about by prior orientation appear to have little effect on the yield stress.

(ii) Draw ratio: Unoriented samples

Values of the natural draw ratio λ_d for unoriented samples of all of the materials examined are given in Table 1. They range from 2.6 for TPI-X to 12 for HDPE-2. Surprisingly, they are consistently larger for the more highly-crystalline materials, whereas one might well have expected the reverse: a greater ductility for less-crystalline materials. Moreover, the largest values are somewhat larger than one would expect for the maximum extensibility of polymer chains in a loose molecular network: rubbery materials will undergo extensions of only up to about 10X at the most, before rupture. As the present materials appear to recover completely on melting, there is no indication of molecular flow during drawing. The molecules thus appear to be retained within a network of entanglements as if they were lightly crosslinked. The high extensibility of HDPE-2 during drawing is therefore quite

surprising, particularly in view of its high degree of crystallinity. A possible model of the drawing process that accounts for these features is advanced in a later section.

(iii) Draw ratio: effect of prior orientation

Values of the draw ratio λ_d for oriented samples of TPI-X and HDPE-1 are plotted in Figure 4 against the prior orientation ratio λ , using logarithmic scales for both axes. As the degree of prior orientation was increased, so the draw ratio decreased, becoming unity; i.e., no drawing took place; when the prior orientation ratio was about 2.4 for TPI-X and about 10 for HDPE-1. On the other hand, when extension was imposed in a direction perpendicular to the prior orientation, i.e., $\lambda < 1$, then the draw ratio increased, reaching values of about 4 for TPI-X and about 14 for HDPE-1.

The variation of λ_d with prior orientation ratio λ was found to be approximately an inverse proportionality: $\lambda_d = \text{constant}/\lambda$. The broken lines in Figure 4 are drawn with a slope of -1, consistent with this relationship. They are seen to describe the experimental results reasonably well, except in the low-orientation region when λ is close to unity. A dependence of this form would arise from the limited extensibility of polymer molecules, because prior orientation by a factor λ would reduce the additional extension ratio λ_d that molecular chains could undergo

before reaching the fully-stretched state, by the factor $\frac{1}{\lambda}$. A treatment of the drawing process in terms of the maximum possible extensibility of polymer molecules is given in the following section.

4. Theoretical Considerations

A simple molecular model of the process of cold drawing in partially-crystalline polymers is now put forward. A representative molecular chain between attachment points to the network, i.e., between molecular entanglements or crosslinks, is shown in Figure 5. It consists of n freely-jointed units, each of length a , so that its fully-stretched length L_m is given by na and its mean end-to-end length L_0 in the molten state, Figure 5a, is given by $n^{1/2}a$. On crystallization the center part of the molecule is assumed to enter a crystallite of length L_c and fold back on itself to enter the same crystallite a number of times, denoted f , Figure 5b. In order for the ends of the molecule, where it is joined to other molecules in the network, to be located on either side of the crystallite, only odd values of f are considered here. In this simple model the degree of crystallization C is given by

$$C = fL_c/L_m \quad (1)$$

It is now assumed that drawing takes place when the molecular chains entering a crystallite apply a sufficiently high stress to it so that it becomes disrupted and transforms into a new extended form, Figure 5c. A further assumption is made that the requisite stress is relatively high so that the molecules are almost fully extended at the onset of crystal rearrangement, and subsequently. Thus, the natural draw ratio λ_d is given by

$$\lambda_d = L_{\pi}/L, \quad (2)$$

where L is the end-to-end distance for a representative chain in the unoriented partially-crystalline state, Figure 5b. This is not necessarily the same as the corresponding distance L_0 in the molten state, Figure 5a. Indeed, it is hypothesized that the process of crystallization will alter the distribution of chain end-to-end distances, $L_0 \rightarrow L$, by excluding junction points from the crystal lattice. In particular, those chains which become fully-extended first on stretching and thus initiate the disruption of crystallites will be those with junction points disposed in the direction of stretching and on either side of a crystallite, as shown schematically in Figure 5b.

An estimate of the initial junction separation distance L can be made as follows. The distance L is composed of a

crystalline sequence length L_c and an amorphous distance L_a , given approximately by the random-coil value $L_a = \frac{L_m}{(1-C)^{1/2} n^{1/2}}$.

Hence,

$$L = L_c + L_a = (CL_m/f) + (1-C)^{1/2} L_m/n^{1/2}, \quad (3)$$

on substituting for L_c in terms of L_m from equation (1).

Thus, the natural draw ratio λ_d is given by

$$1/\lambda_d = (C/f) + (1-C)^{1/2}/n^{1/2}, \quad (4)$$

from equations 2 and 3.

This simple treatment suggests that the natural draw ratio will be large for materials in which the molecules re-enter the crystallites many times and f is large, even when the degree of crystallization is high. In other circumstances, the predicted draw ratio is small. Two extreme cases are now considered. In each case the number n of random links per molecular strand is given the representative value, 200.

For TPI-X, the degree of crystallinity C is 36 percent and the natural draw ratio is about 2.6, Table 1. From equation 4, the average number of times f that a chain passes through a crystallite is obtained as 1.1, indicating that for this material there is relatively little re-entry or chain-folding. For HDPE-2, on the other hand, the degree of crystallinity is 72 percent and the natural draw ratio is about 12. From equation 4 the average number of times f

that a molecular chain passes through a single crystallite is obtained as 15.6, indicating that there is a great deal of re-entry or folded-chain crystallization in HDPE-2, as prepared here.

From the number of random links involved in crystalline sequences, 72 for TPI-X and 144 for HDPE-2, and the inferred number of times that each chain enters the same crystallite, we may deduce the mean length \bar{L}_c of a crystallite to be 65 random links for TPI-X and 9.2 random links for HDPE-2. The latter number is consistent with the known crystal microstructure of polyethylene, corresponding to about 5-10 nm, but the value for TPI-X seems unacceptably high. It should be noted, however, that the present analysis does not distinguish between a chain passing through a single crystalline sequence in the direction of stretching or a chain passing through two or more crystalline sequences, without reversing direction, before a junction point is reached. Thus, the large number of random links deduced for the crystalline sequence length in TPI-X may in reality be the sum of several crystallite lengths traversed by the same molecular strand. Nevertheless, a clear implication of the present analysis is that chain-folding is much less prominent in TPI-X and that the crystallites are considerably longer (thicker) than in HDPE. It would be interesting and worthwhile to examine other partially-

crystalline polymers and to make direct comparison with their crystallite thicknesses, determined, for example, by SAXS.

The large effect of prior orientation upon the draw ratio λ_d , discussed previously and shown in Figure 4, can be interpreted in terms of the molecular model advanced here. It is in accord with a continuous change in the chain end -to-end length L with prior orientation, as might well be expected, with a corresponding reduction in the number of times that a molecular strand traverses a single crystallite.

5. Effect of Annealing or Quenching

A direct implication of the analysis given here is that an increase in crystallite thickness, brought about by annealing, for example, should result in fewer re-entries and a decrease in the natural draw ratio. Conversely, a decrease in crystallite thickness and corresponding increase in number of molecular re-entries should cause an increase in natural draw ratio. Unoriented samples of HDPE-1 and TPI-X were therefore prepared by melting sheets and allowing them to crystallize at different temperatures so that the crystallite layer thicknesses would be somewhat different. Values of the natural draw ratio are given in Table 2. As can be seen, the higher the temperature T_c of crystallization (and, hence, the thicker the crystallite), the lower ^{is} λ_d the natural draw ratio λ_d , in general. This trend is in accord with the mechanism of cold drawing put forward here.

6. Conclusions

Measurements have been made of the tensile properties of several representative partially-crystalline polymers, crystallized both in the oriented and unoriented state. The yield stress was found to be virtually unchanged by prior orientation but the natural draw ratio decreased in inverse proportion to the amount of preorientation.

Striking differences were found between the natural draw ratio for various polymers. A simple molecular model for the drawing process was developed in terms of a loose network of molecules, held together by entanglements or crosslinks which are excluded from the crystal lattice. As a result, the end-to-end distance for molecular strands in the partially-crystalline material is different from that in the melt. Under tension, certain strands become fully-stretched and initiate disruption of the crystallites, followed by their rearrangement into the fully-drawn state. The principal term in the analysis appears to be the number of times that a molecule reverses direction and re-enters the same crystallite. When this is large, the natural draw ratio is large also.

This simple concept accounts successfully for the major features of cold drawing: large differences between different materials, a continuous decrease in the natural draw ratio with the extent of prior extension in the melt, and a decrease in the natural draw ratio on annealing.

Acknowledgements

This work was carried out in part while one of the authors (A.N.G.) was a Visiting Scientist at the Institut de Genie des Materiaux, National Research Council of Canada, Boucherville, Quebec. Kind hospitality of the Director, G. Bata, and the Plastics Research Group, led by Professor J.-M. Charrier, is gratefully acknowledged. It forms part of a program of research supported by a grant from the Office of Naval Research (Contract N00014-76-C-0408), and a grant-in-aid from Cabot Corporation.

References

1. P.I. Vincent, *Polymer*, 1, 7 (1960).
2. A. Peterlin and H.G. Olf, *J. Polym. Sci., Part A-2*, 4, 587 (1966).
3. G. Capaccio, T.A. Crompton and I.M. Ward, *J. Polym. Sci.: Polym. Phys. Ed.*, 14, 1461 (1976).
4. L. Mandelkern, *Chem. Rev.*, 56, 903 (1956).
5. A.P. Gray, *Thermochim. Acta*, 1, 563 (1970).
6. R. Chiang and P.J. Flory, *J. Am. Chem. Soc.*, 83, 2857 (1961).

Table 1. Physical properties of the materials examined

Material	Density \underline{d} (kg/m ³)	Crystallinity \underline{C} (%)	Yield Stress $\underline{\sigma}_y$ (MPa)	Draw Ratio \underline{d}
TPI-X		36*	9.0	2.6
TPI		37*	9.0	2.7
LDPE		50*	10.5	5
MDPE	940	62**	21.5	7
HDPE-1		64*	24	8.6
HDPE-2	955	72**	29	12

* Measured by DSC with a heating rate of 0.17 C/s.
Reported values for 100% crystallinity are: 44.5 cal/g
for TPI (4) and 69 cal/g for polyethylene (5).

** C was calculated from the measured density using a relation
given by Chiang and Flory (6).

Table 2. Natural draw ratio λ_d for quenched and annealed samples.

Crystallization temperature, T_c ($^{\circ}\text{C}$)		λ_d
	<u>TPI-X</u>	
0		2.6
40		2.4
45		2.1
	<u>LDPE</u>	
Quenched ($T_c = 20-90\text{ C}$)		4.8
100		5.3
	<u>MDPE</u>	
Quenched ($T_c = 20-100\text{ C}$)		6.4
118		7.7
	<u>HDPE-1</u>	
Quenched ($T_c = 20-100\text{ C}$)		8.6
115		7.0
121		3.5
	<u>HDPE-2</u>	
Quenched ($T_c = 20-100\text{ C}$)		10.5
115		11.0
121		3.0

Figure Legends

- Figure 1. Relations between tensile stress $\underline{\sigma}$ and apparent extension \underline{e} for oriented samples of HDPE-1.
- Figure 2. Relations between tensile stress $\underline{\sigma}$ and apparent extension \underline{e} for oriented samples of TPI-X.
- Figure 3. Dependence of yield stress $\underline{\sigma}_y$ upon the prior orientation extension ratio $\underline{\lambda}$ in the stretching direction, for HDPE-1, ●, and TPI-X, ○.
- Figure 4. Dependence of natural draw ratio $\underline{\lambda}_d$ upon the prior orientation extension ratio $\underline{\lambda}$ in the stretching direction, for HDPE-1, ●, and TPI-X, ○. The broken lines are drawn with a slope of -1.
- Figure 5. (a) Sketch of a molecular strand between tie points in the melt.
(b) In the crystalline state.
(c) In the drawn state.

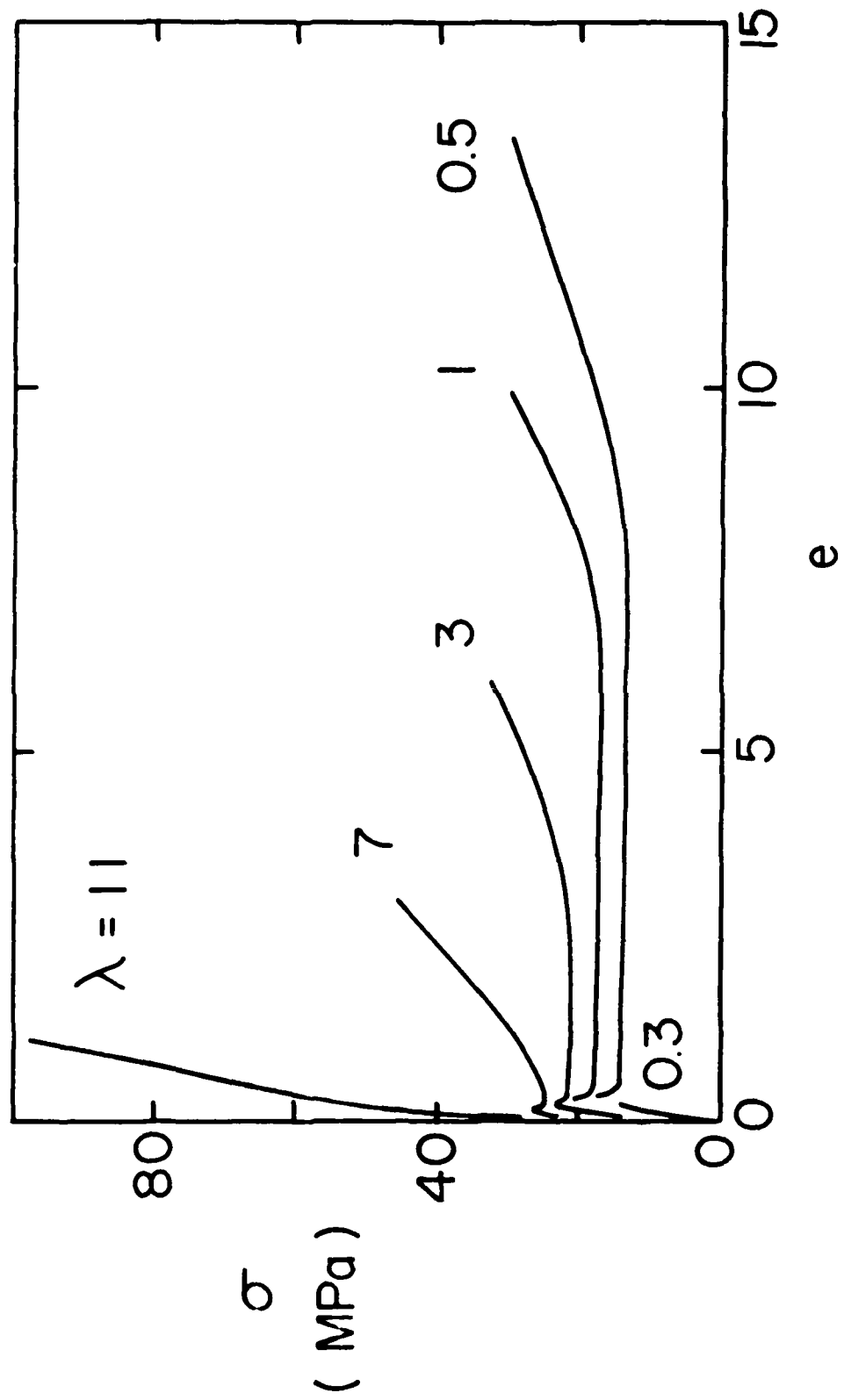


Figure 1

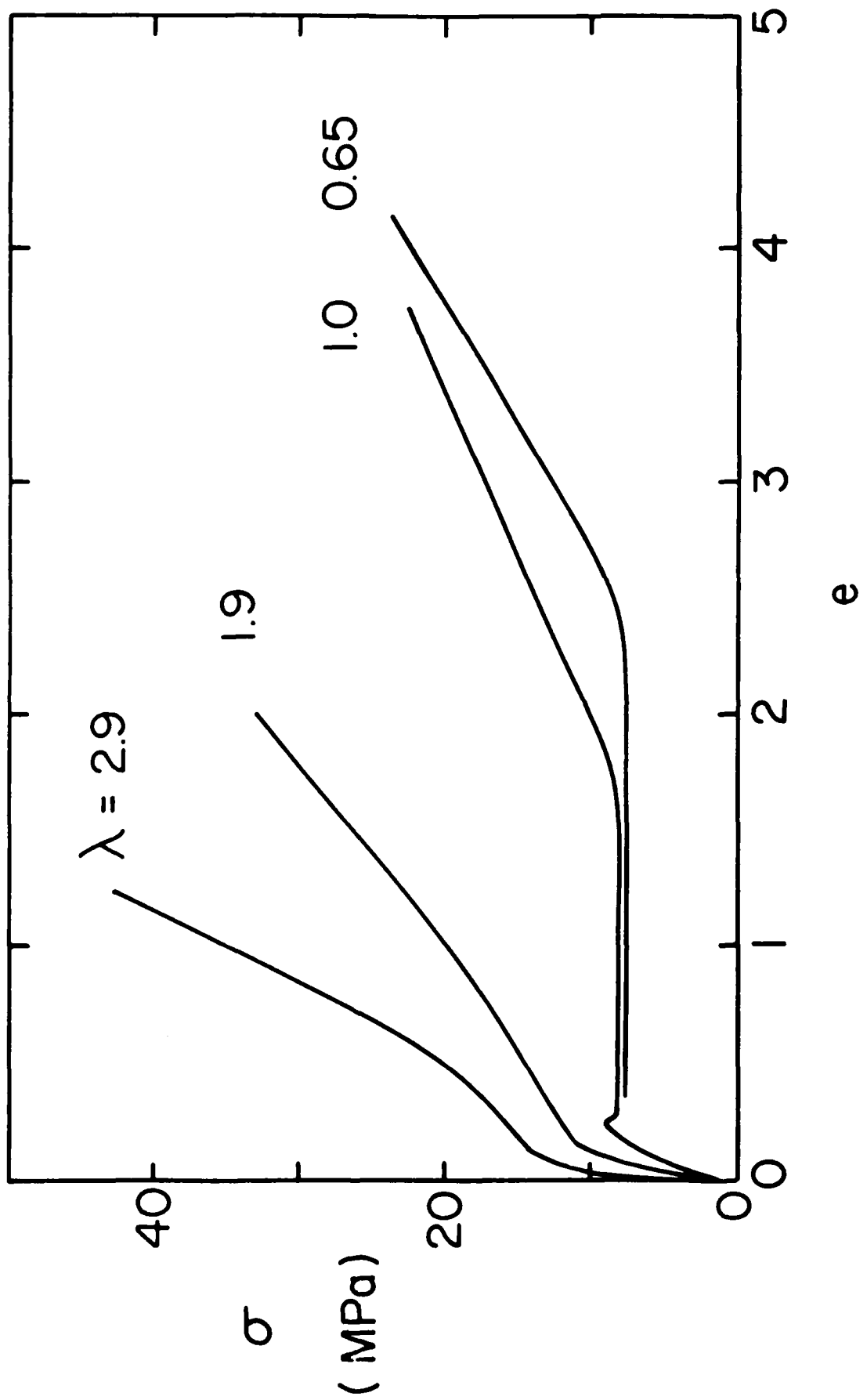


Figure 2

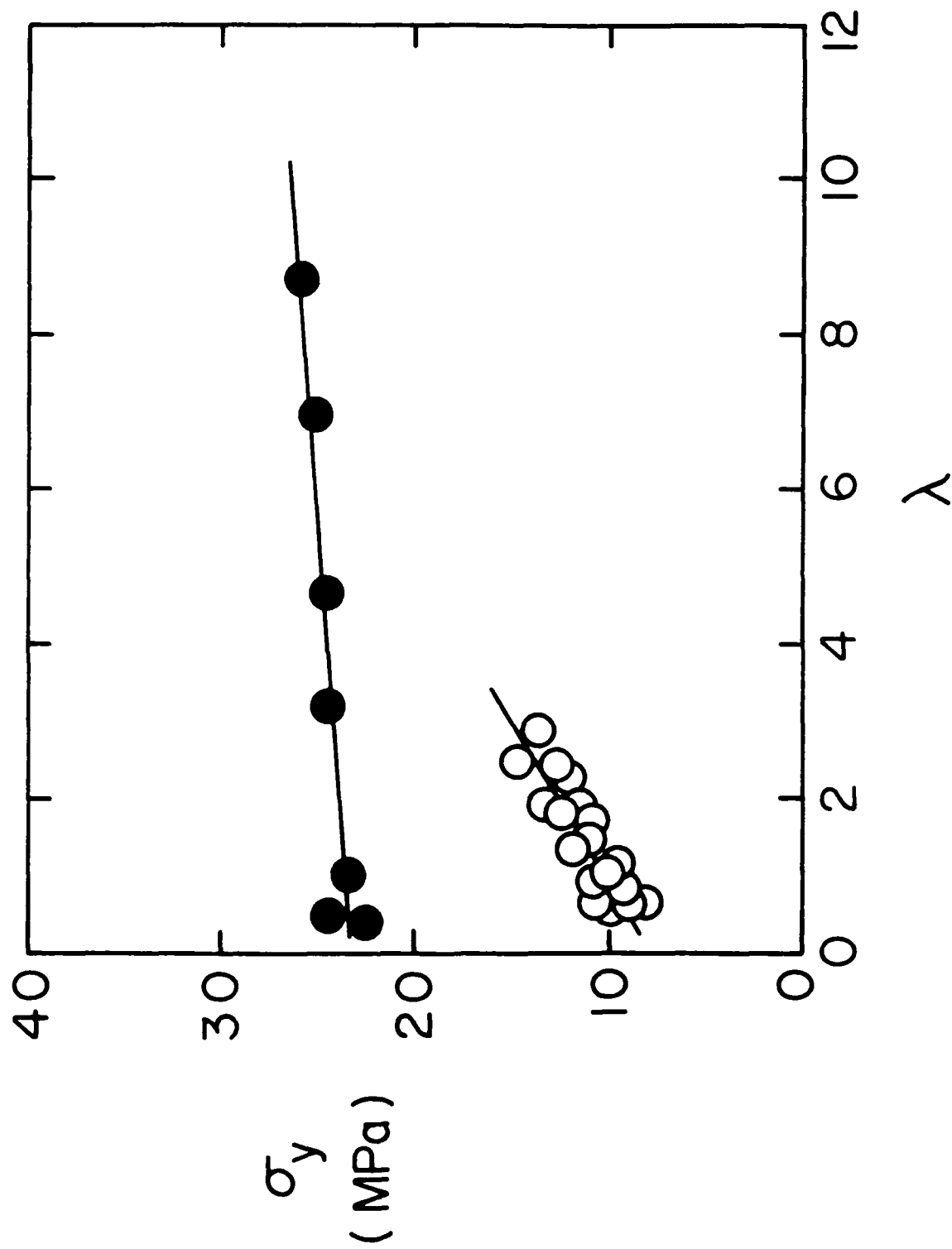


Figure 3

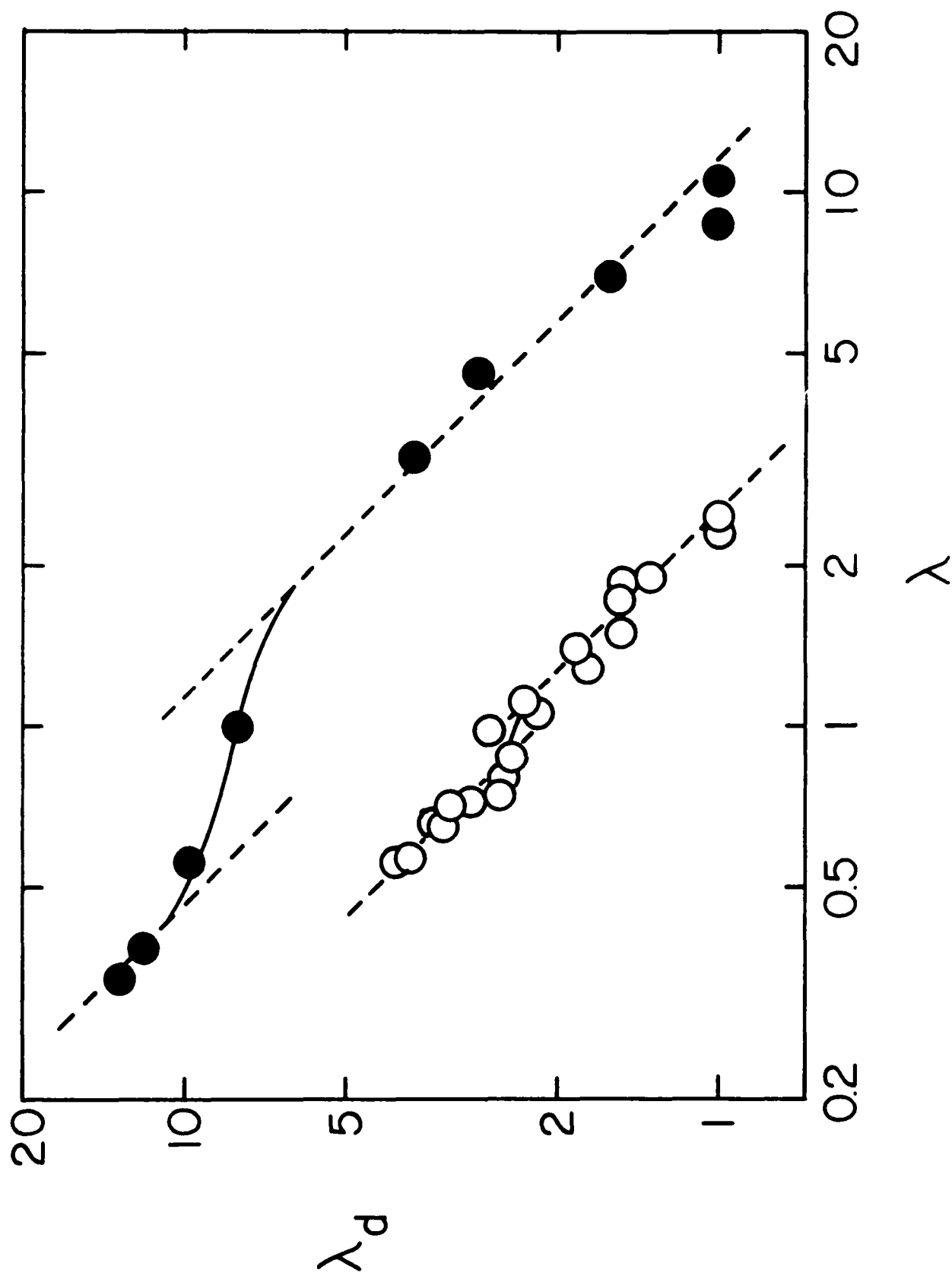
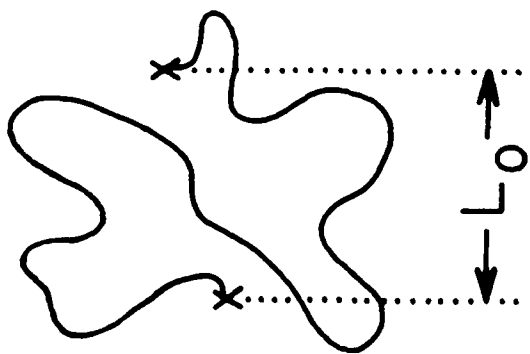
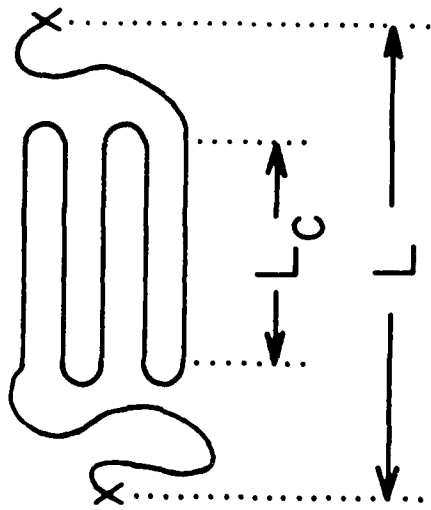


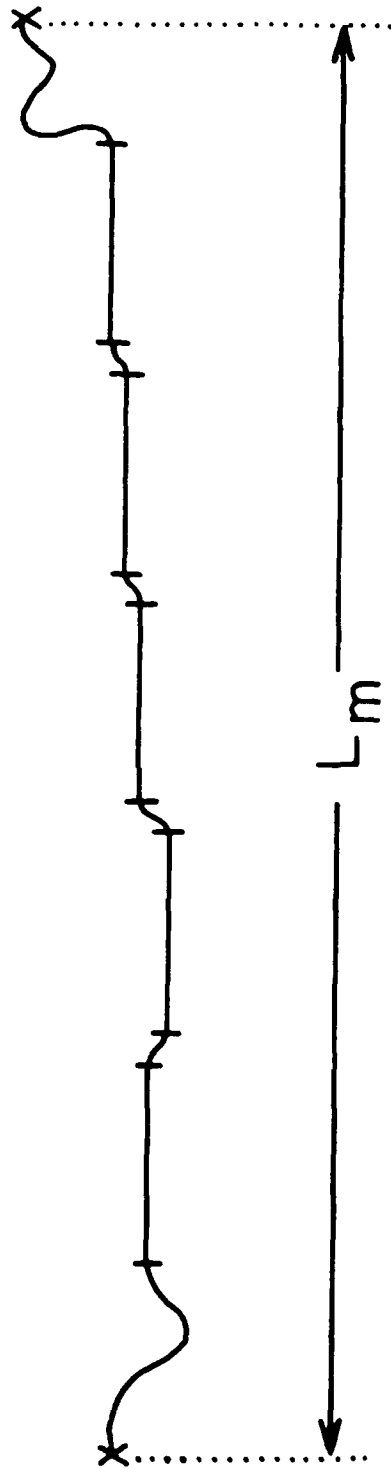
Figure 4



(a)



(b)



(c)

Figure 5

(DYN)

DISTRIBUTION LIST

Dr. R.S. Miller
Office of Naval Research
Code 432P
Arlington, VA 22217
(10 copies)

Dr. J. Pastine
Naval Sea Systems Command
Code 06R
Washington, DC 20362

Dr. Kenneth D. Hartman
Hercules Aerospace Division
Hercules Incorporated
Alleghany Ballistic Lab
P.O. Box 210
Washington, DC 21502

Mr. Otto K. Heiney
AFATL-DLJG
Elgin AFB, FL 32542

Dr. Merrill K. King
Atlantic Research Corp.
5390 Cherokee Avenue
Alexandria, VA 22312

Dr. R.L. Lou
Aerojet Strategic Propulsion Co.
Bldg. 05025 - Dept 5400 - MS 167
P.O. Box 15699C
Sacramento, CA 95813

Dr. R. Olsen
Aerojet Strategic Propulsion Co.
Bldg. 05025 - Dept 5400 - MS 167
P.O. Box 15699C
Sacramento, CA 95813

Dr. Randy Peters
Aerojet Strategic Propulsion Co.
Bldg. 05025 - Dept 5400 - MS 167
P.O. Box 15699C
Sacramento, CA 95813

Dr. D. Mann
U.S. Army Research Office
Engineering Division
Box 12211
Research Triangle Park, NC 27709-2211

Dr. L.V. Schmidt
Office of Naval Technology
Code 07CT
Arlington, VA 22217

JHU Applied Physics Laboratory
ATTN: CPIA (Mr. T.W. Christian)
Johns Hopkins Rd.
Laurel, MD 20707

Dr. R. McGuire
Lawrence Livermore Laboratory
University of California
Code L-324
Livermore, CA 94550

P.A. Miller
736 Leavenworth Street, #6
San Francisco, CA 94109

Dr. W. Moniz
Naval Research Lab.
Code 6120
Washington, DC 20375

Dr. K.F. Mueller
Naval Surface Weapons Center
Code R11
White Oak
Silver Spring, MD 20910

Prof. M. Nicol
Dept. of Chemistry & Biochemistry
University of California
Los Angeles, CA 90024

Mr. L. Roslund
Naval Surface Weapons Center
Code R10C
White Oak, Silver Spring, MD 20910

Dr. David C. Sayles
Ballistic Missile Defense
Advanced Technology Center
P.O. Box 1500
Huntsville, AL 35807

(DYN)

DISTRIBUTION LIST

Mr. R. Geisler
ATTN: DY/MS-24
AFRPL
Edwards AFB, CA 93523

Naval Air Systems Command
ATTN: Mr. Bertram P. Sobers
NAVAIR-320G
Jefferson Plaza 1, RM 472
Washington, DC 20361

R.B. Steele
Aerocjet Strategic Propulsion Co.
P.O. Box 15699C
Sacramento, CA 95813

Mr. M. Stosz
Naval Surface Weapons Center
Code R10P
White Oak
Silver Spring, MD 20910

Mr. E.S. Sutton
Thiokol Corporation
Elkton Division
P.O. Box 241
Elkton, MD 21921

Dr. Grant Thompson
Morton Thiokol, Inc.
Wasatch Division
MS 240 P.O. Box 524
Brigham City, UT 84302

Dr. R.S. Valentini
United Technologies Chemical Systems
P.O. Box 50015
San Jose, CA 95150-0015

Dr. R.F. Walker
Chief, Energetic Materials Division
DRSMC-LCE (D), B-3022
USA ARDC
Dover, NJ 07801

Dr. Janet Wall
Code 012
Director, Research Administration
Naval Postgraduate School
Monterey, CA 93943

Director
US Army Ballistic Research Lab.
ATTN: DRXBR-IBD
Aberdeen Proving Ground, MD 21005

Commander
US Army Missile Command
ATTN: DRSMI-RKL
Walter W. Wharton
Redstone Arsenal, AL 35898

Dr. Ingo W. May
Army Ballistic Research Lab.
ARRADCOM
Code DRXBR - IBD
Aberdeen Proving Ground, MD 21005

Dr. E. Zimet
Office of Naval Technology
Code 071
Arlington, VA 22217

Dr. Ronald L. Derr
Naval Weapons Center
Code 389
China Lake, CA 93555

T. Boggs
Naval Weapons Center
Code 389
China Lake, CA 93555

Lee C. Estabrook, P.E.
Morton Thiokol, Inc.
P.O. Box 30058
Shreveport, Louisiana 71130

Dr. J.R. West
Morton Thiokol, Inc.
P.O. Box 30058
Shreveport, Louisiana 71130

Dr. D.D. Dillehay
Morton Thiokol, Inc.
Longhorn Division
Marshall, TX 75670

G.T. Bowman
Atlantic Research Corp.
7511 Wellington Road
Gainesville, VA 22065

(DYN)

DISTRIBUTION LIST

R.E. Shenton
Atlantic Research Corp.
7511 Wellington Road
Gainesville, VA 22065

Mike Barnes
Atlantic Research Corp.
7511 Wellington Road
Gainesville, VA 22065

Dr. Lionel Dickinson
Naval Explosive Ordnance
Disposal Tech. Center
Code D
Indian Head, MD 20340

Prof. J.T. Dickinson
Washington State University
Dept. of Physics 4
Pullman, WA 99164-2814

M.H. Miles
Dept. of Physics
Washington State University
Pullman, WA 99164-2814

Dr. T.F. Davidson
Vice President, Technical
Morton Thiokol, Inc.
Aerospace Group
110 North Wacker Drive
Chicago, Illinois 60606

Mr. J. Consaga
Naval Surface Weapons Center
Code R-16
Indian Head, MD 20640

Naval Sea Systems Command
ATTN: Mr. Charles M. Christensen
NAVSEA-62R2
Crystal Plaza, Bldg. 6, Rm 806
Washington, DC 20362

Mr. R. Beauregard
Naval Sea Systems Command
SEA 64E
Washington, DC 20362

Brian Wheatley
Atlantic Research Corp.
7511 Wellington Road
Gainesville, VA 22065

Mr. G. Edwards
Naval Sea Systems Command
Code 62R32
Washington, DC 20362

C. Dickinson
Naval Surface Weapons Center
White Oak, Code R-13
Silver Spring, MD 20910

Prof. John Deutch
MIT
Department of Chemistry
Cambridge, MA 02139

Dr. E.H. deButts
Hercules Aerospace Co.
P.O. Box 27408
Salt Lake City, UT 84127

David A. Flanigan
Director, Advanced Technology
Morton Thiokol, Inc.
Aerospace Group
110 North Wacker Drive
Chicago, Illinois 60606

Dr. L.H. Caveny
Air Force Office of Scientific
Research
Directorate of Aerospace Sciences
Bolling Air Force Base
Washington, DC 20332

W.G. Roger
Code 5253
Naval Ordnance Station
Indian Head, MD 20640

Dr. Donald L. Ball
Air Force Office of Scientific
Research
Directorate of Chemical &
Atmospheric Sciences
Bolling Air Force Base
Washington, DC 20332

(DYN)

DISTRIBUTION LIST

Dr. Anthony J. Matuszko
Air Force Office of Scientific Research
Directorate of Chemical & Atmospheric
Sciences
Bolling Air Force Base
Washington, DC 20332

Dr. Michael Chaykovsky
Naval Surface Weapons Center
Code R11
White Oak
Silver Spring, MD 20910

J.J. Rocchio
USA Ballistic Research Lab.
Aberdeen Proving Ground, MD 21005-5066

G.A. Zimmerman
Aerojet Tactical Systems
P.O. Box 13400
Sacramento, CA 95813

B. Swanson
INC-4 MS C-346
Los Alamos National Laboratory
Los Alamos, New Mexico 87545

Dr. James T. Bryant
Naval Weapons Center
Code 3205B
China Lake, CA 93555

Dr. L. Rothstein
Assistant Director
Naval Explosives Dev. Engineering Dept.
Naval Weapons Station
Yorktown, VA 23691

Dr. M.J. Kamlet
Naval Surface Weapons Center
Code R11
White Oak, Silver Spring, MD 20910

Dr. Henry Webster, III
Manager, Chemical Sciences Branch
ATTN: Code 5063
Crane, IN 47522

Dr. A.L. Slafkosky
Scientific Advisor
Commandant of the Marine Corps
Code RD-1
Washington, DC 20380

Dr. H.G. Adolph
Naval Surface Weapons Center
Code R11
White Oak
Silver Spring, MD 20910

U.S. Army Research Office
Chemical & Biological Sciences
Division
P.O. Box 12211
Research Triangle Park, NC 27709

G. Butcher
Hercules, Inc.
MS X2H
P.O. Box 98
Magna, Utah 84044

W. Waesche
Atlantic Research Corp.
7511 Wellington Road
Gainesville, VA 22065

Dr. John S. Wilkes, Jr.
FJSRL/NC
USAF Academy, CO 80840

Dr. H. Rosenwasser
AIR-320R
Naval Air Systems Command
Washington, DC 20361

Dr. Joyce J. Kaufman
The Johns Hopkins University
Department of Chemistry
Baltimore, MD 21218

Dr. A. Nielsen
Naval Weapons Center
Code 385
China Lake, CA 93555

(DYN)

DISTRIBUTION LIST

K.D. Pae
High Pressure Materials Research Lab.
Rutgers University
P.O. Box 909
Piscataway, NJ 08854

Prof. Edward Price
Georgia Institute of Tech.
School of Aerospace Engineering
Atlanta, GA 30332

Dr. John K. Dienes
T-3, B216
Los Alamos National Lab.
P.O. Box 1663
Los Alamos, NM 87544

J.A. Birkett
Naval Ordnance Station
Code 5253K
Indian Head, MD 20640

A.N. Gent
Institute Polymer Science
University of Akron
Akron, OH 44325

Prof. R.W. Armstrong
University of Maryland
Dept. of Mechanical Engineering
College Park, MD 20742

Dr. D.A. Shockey
SRI International
333 Ravenswood Ave.
Menlo Park, CA 94025

Herb Richter
Code 385
Naval Weapons Center
China Lake, CA 93555

Dr. R.B. Kruse
Morton Thiokol, Inc.
Huntsville Division
Huntsville, AL 35807-7501

J.T. Rosenberg
SRI International
333 Ravenswood Ave.
Menlo Park, CA 94025

G. Butcher
Hercules, Inc.
P.O. Box 98
Magna, UT 84044

G.A. Zimmerman
Aeroject Tactical Systems
P.O. Box 13400
Sacramento, CA 95813

W. Waesche
Atlantic Research Corp.
7511 Wellington Road
Gainesville, VA 22065

Prof. Kenneth Kuo
Pennsylvania State University
Dept. of Mechanical Engineering
University Park, PA 16802

Dr. R. Bernecker
Naval Surface Weapons Center
Code R13
White Oak
Silver Spring, MD 20910

T.L. Boggs
Naval Weapons Center
Code 3891
China Lake, CA 93555

(DYN)

DISTRIBUTION LIST

Dr. C.S. Coffey
Naval Surface Weapons Center
Code R13
White Oak
Silver Spring, MD 20910

D. Curran
SRI International
333 Ravenswood Avenue
Menlo Park, CA 94025

E.L. Throckmorton
Code SP-2731
Strategic Systems Program Office
Crystal Mall #3, RM 1048
Washington, DC 20376

Dr. R. Martinson
Lockheed Missiles and Space Co.
Research and Development
3251 Hanover Street
Palo Alto, CA 94304

C. Gotzmer
Naval Surface Weapons Center
Code R-11
White Oak
Silver Spring, MD 20910

G.A. Lo
3251 Hanover Street
B204 Lockheed Palo Alto Research Lab
Palo Alto, CA 94304

R.A. Schapery
Civil Engineering Department
Texas A&M University
College Station, TX 77843

J.M. Culver
Strategic Systems Projects Office
SSPO/SP-2731
Crystal Mall #3, RM 1048
Washington, DC 20376

Prof. G.D. Duvall
Washington State University
Department of Physics
Pullman, WA 99163

Dr. E. Martin
Naval Weapons Center
Code 3858
China Lake, CA 93555

Dr. M. Farber
135 W. Maple Avenue
Monrovia, CA 91016

W.L. Elban
Naval Surface Weapons Center
White Oak, Bldg. 343
Silver Spring, MD 20910

G.E. Manser
Morton Thickett
Wasatch Division
P.O. Box 524
Brigham City, UT 84302

R.G. Rosemeier
Brimrose Corporation
7720 Belair Road
Baltimore, MD 20742

Ser 432/84/340
Revised January 1985

Administrative Contracting
Officer (see contract for
address)
(1 copy)

Director
Naval Research Laboratory
Attn: Code 2627
Washington, DC 20375
(6 copies)

Defense Technical Information Center
Bldg. 5, Cameron Station
Alexandria, VA 22314
(12 copies)

Dr. Robert Polvani
National Bureau of Standards
Metallurgy Division
Washington, D.C. 20234

Dr. Y. Gupta
Washington State University
Department of Physics
Pullman, WA 99163

END

FILMED

4-85

DTIC

